ResearchGate

See discussions, stats, and author profiles for this publication at: https://www.researchgate.net/publication/237017556

SAR study and conformational analysis of a series of novel peptide G protein-coupled receptor kinase 2 (GRK2) inhibitors.

ARTICLE *in* BIOPOLYMERS · JANUARY 2014

Impact Factor: 2.39 · DOI: 10.1002/bip.22295 · Source: PubMed

CITATIONS
3

READS
59

13 AUTHORS, INCLUDING:

Isabel M Gomez-Monterrey
University of Naples Federico II
98 PUBLICATIONS **1,906** CITATIONS
SEE PROFILE

Alfonso Carotenuto
University of Naples Federico II
96 PUBLICATIONS **1,062** CITATIONS
SEE PROFILE

Paolo Grieco
University of Naples Federico II
174 PUBLICATIONS **2,294** CITATIONS
SEE PROFILE

Pietro Campiglia
Università degli Studi di Salerno
142 PUBLICATIONS **1,286** CITATIONS
SEE PROFILE

Available from: Isabel M Gomez-Monterrey
Retrieved on: 13 January 2016

Accepted Article

SAR study and conformational analysis of a series of novel peptide G protein–coupled receptor kinase 2 (GRK2) inhibitors

Isabel Gomez–Monterrey,[1,†] Alfonso Carotenuto,[1,†] Ersilia Cipolletta,[2,†] Marina Sala,[3] Ermelinda Vernieri,[3] Antonio Limatola,[1] Alessia Bertamino,[3] Simona Musella,[3] Paolo Grieco,[1] Bruno Trimarco,[2] Ettore Novellino,[1] Guido Iaccarino,[4,5,*] Pietro Campiglia[3,*]

[1] Department of Pharmacy, "Federico II" University of Naples, Italy. [2] Department of Clinical Medicine and Cardiovascular and Immunological Science, "Federico II" University of Naples, Italy. [3] Department of Pharmaceutical Science, University of Salerno, Italy. [4] Department of Medicine and Surgery, University of Salerno, Italy. [5] IRCCS, "Multimedica", Milano, Italy

[†]These authors contributed equally to the work

* To whom correspondence should be addressed:

Prof. Guido Iaccarino; of Medicine and Surgery, University of Salerno, Salerno, Italy. phone, +39-089-965021; Email, giaccarino@unisa.it.

Prof. Pietro Campiglia; Pharmaceutical Science, University of Salerno, Salerno, Italy. phone +39-089-969242; Email: pcampigl@unisa.it

This article has been accepted for publication and undergone full peer review but has not been through the copyediting, typesetting, pagination and proofreading process which may lead to differences between this version and the Version of Record. Please cite this article as an 'Accepted Article', doi: 10.1002/bip.22295
© 2013 Wiley Periodicals, Inc.

ABSTRACT

G protein-coupled receptor kinase 2 (GRK2) plays a central role in the cellular transduction network. In particular, during chronic heart failure GRK2 is upregulated and believed to contribute to desease progression. Thereby, its inhibition offers a potential therapeutic solution to several pathological conditions. In the present study, we performed a SAR study and a NMR conformational analysis of peptides derived from HJ loop of GRK2 and able to selectively inhibit GRK2. Fron Ala-scan and *D*-Ala point replacement, we found that Arg residues don't affect the inhibitory properties, while a *D*-amino acid at position 5 is key to the activity. Conformational analysis identified two β-turns that involve N-terminal residues, followed by a short extended region. These information can help the design of peptides and peptido-mimetics with enhanced GRK2 inhibition properties.

KEYWORDS: GRK2 inhibitors; cardiovascular system; peptide Ala-scan; NMR conformational analysis.

Accepted Article

Accepted Article

INTRODUCTION

The G protein-coupled receptor kinase family (GRKs) constitutes a group of seven protein kinases that specifically recognize and phosphorylate agonist-activated G protein-coupled receptors (GPCRs).[1] GRKs-mediated receptor phosphorylation triggers the binding of arrestin proteins that uncouple receptors from G proteins leading to rapid desensitization.[2-4] As a result of β-arrestin binding, phosphorylated receptors are also targeted for clathrin-mediated endocytosis, a process that classically serves to re-sensitize and recycle receptors back to the plasma membrane.[5] The seven mammalian members of the GRK family can be divided into three subfamilies based on sequence and functional similarity: visual GRK subfamily (GRK1 and GRK7), the β-adrenergic receptor kinase (GRK2/ GRK3), and the GRK4 subfamily (GRK4, GRK5 and GRK6).[1, 6, 7] All GRKs share a common structural architecture that includes an N-terminal regulator of G protein signalling homology domain (RH), a central kinase catalytic domain, and a C-terminal region containing a pleckstrin homology domain (PH).[1,8] The best characterized member of this family is the ubiquitously expressed GRK2, also known as β-adrenergic receptor kinase 1 (β-ARK1).[8,9] In the past 20 years, GRK2 emerges as a key node in signal transduction pathway playing a major role in the agonist-specific desensitization of several metabolism-related GPCRs, including the β-adrenergic, melanocortin, endothelin, and glucose-dependent insulinotropic polypeptide receptors.[9,10,11] GRK2 can also phosphorylate other membrane receptors[9,12] as well as non-receptor substrates,[9,11] acting as effector in the regulation of diverse cellular phenomena from cardiovascular and immune cell functionality to migration and cell cycle progression.[9,13-16] Furthermore, GRK2 may also contribute to modulate cellular responses in a phosphorylation-independent manner thank to its ability to interact with a plethora of proteins involved in signaling and trafficking.[5,17] All these functional interactions predicts that alterations in GRK2 levels and/or activity may have important effects in human diseases,[9,18] as those reported in several relevant cardiovascular,[19-24] inflammatory,[25] or cancer pathologies.[9,26,27,28]

Accepted Article

In the last year, identification of GRK2 modulators/inhibitors are very active fields of research. Different small molecules inhibitors of GRK2 activity are currently available, even if they are characterized by low sensitivity and specificity.[29-32] Strategies to selectively inhibit the GRK2 activity have been attempted using shorter peptides [33-35] or RNA aptamers.[36] In particular, Anis et al.[35] demonstrated that myristyl or lauryl glycine derivatives of short peptides derived from HJ loop of GRK2, such as KRX-683_{107} and KRX-683_{124} (Table 1), are potent inhibitor of the kinase and possess hypoglycemic effect in animal models of Type 2 diabetes. The peptide fragments of these compounds closely resemble the catalytic fragment 383-390 KLLRGHSP of GRK2. This fragment is composed by the last part of the α-helix F (residues 383-386) and the first part of a strand (residues 387-390) within the HJ loop. Several crystallographic and mutational studies, have pointed to HJ-αG residues as being involved in substrate binding and in binding to upstream activators.[33,34] Based on these findings, this fragment and, more concretely, compounds **1** and **2** appeared to be valuable starting points for the development of novel specific and more potent GRK2 inhibitors.

In this work we first describe the structure-activity relationship (SAR) of peptides **1** and **2** based on an Ala-scan analysis. A detailed conformational study by NMR techniques and the biological effects of GRK2 inhibition for the most potent derivatives characterized in this work was also discussed.

RESULTS

Synthesis and biological activity.

In a first classical approach, a series of *L*-Ala-substituted analogues of peptides **1** and **2**, were synthesized in order to evaluate the amino acid side chains involved in the interaction with the target molecule (**3-15**, Table 2, and Table S1 of the Supporting Information). To verify the effect of chirality, the *D*-Arg at position 5 was also replaced by *D*-Ala (**16** and **17**). Peptides **1-17** were synthesized by standard 9-fluorenylmethoxy carbonyl (Fmoc) chemistry using an appropriate orthogonal protection strategy.[37]

The effectiveness of these peptides to inhibit GRK2 kinase activity was assessed by in vitro assay using GRK2 (or GRK5, see below) purified protein and the G protein–coupled receptor rod outer segments (ROS) as a substrate (Table 2) in presence of [γ-^{32}P]- adenosine triphosphate (ATP). Phosphorylation of rhodopsin by GRK5 and GRK2 occurs on serine and threonine residues within the C-terminal 19 amino acids.[38] Interestingly, the serine residues phosphorylated by these different GRKs are essentially identical, principally Ser-338 and Ser-343, although it has been shown that GRK5 preferentially phosphorylate Ser-338, whereas GRK2 preferentially phosphorylate Ser-343.[39] Peptide **1** causes a 47.6±5.5% inhibition of GRK2 activity on ROS; within the sequence of **1**, the amino acids Leu2, Leu3, and *D*-Arg5 are relevant for the inhibitory properties of the reference peptide. Also C-terminal residues proved to be important, since Ala replacement of His6 and Ser7 led to about three and two-fold reduction of the inhibitory activity. As in the original sequence the amino acid in position 5 is a *D*-enantiomer (*D*-Arg), we also substitute this amino acid with a *D*-Ala (peptide **16**) in order to discern the real role of molecular orientation from the effects of the amino acid side chain on the inhibitory activity. We found that indeed, substitution with a neutral *D*-amino acid such as alanine maintained the inhibitory properties of the resulting peptide **16** (55.5±4.7%).

A similar approach was assessed for peptide **2**. First of all, **2** causes a 49.6±6.3% decrease in GRK2 activity. Ala substitution in position Leu2, Leu3 and Arg4 (peptides **9**, **10**, and **11**) does not change the inhibitory property of the parent peptide **2**. On the contrary, changes of residues *D*-Arg5, His6, Ser7, and Ile8 lead to compounds (**12**, **13**, **14,** and **15**) that are devoid of inhibitory activity. Similarly to peptide **1**, the reinstallation of *D*- chirality in residue 5 restores the inhibitory properties of resulting peptide **17** on GRK2 (63.2±9.7%) which showed the highest GRK2 inhibition potency of the series.

To test the specificity of the peptides for GRK2 rather than for the substrate, we also repeated the same experiment using as substrate Myelin Basic Protein (MBP). MBP is an ideal model substrate, since this basic protein can be phosphorylated at multiple sites (Ser-11, Ser-55, Ser-8, Ser-132, Ser-55, Ser-161, and Ser-46) from several kinase types.[40] Therefore, in this study we have used the

Accepted Article

myelin basic protein as conventional substrate for in vitro kinase assay. With this substrate, we observed a similar inhibition pattern as for ROS (Table 2).

Next, to verify whether these peptides selectively inhibit GRK2, we repeated the activity assay substituting GRK5 to GRK2 purified protein. GRK2 selective inhibition is suggested by the evidence that all peptides don't affect GRK5 kinase activity on rhodopsin or MBP phosphorylation levels (Table 2).

To verify the effectiveness of GRK2 inhibition in a cellular contest, we tested the effects of GRK2 inhibitors in cells on the cyclic adenosine monophosphate (cAMP) production. In Hek293 cells stably overexpressing the β_2 adrenergic receptor (β_2AR),[12] incubation with compounds **1**, **2**, and **17** resulted in a slight increment of basal and βAR stimulated cAMP production in HEK-293 cells (Figure 1). Interestingly, the lead compound **2** appears to be the most effective in this assay.

NMR analysis of selected peptides.

NMR analysis of peptides **1**, **2**, **16**, and **17** was performed in water and dodecylphosphocholine (DPC) micelle solutions. Almost complete ^{1}H NMR chemical shift assignments (Supporting Information, Tables S2-S9) were achieved according to the Wüthrich procedure[41] via the usual systematic application of Total Correlation Spectroscopy (TOCSY), and Nuclear Overhauser Effect Spectroscopy (NOESY) experiments in both environments. Considering the spectra in water solution, all NMR parameters indicated structural flexibility (Tables S2-S5). For example, no standard α-helix or β-sheet structure from H_α CSI (chemical shift index) values,[42] and no unambiguous medium- or long-range backbone NOE connectivities were found in the NOESY spectrum of the peptides. Only strong $d_{\alpha N}$(i, i+1) NOEs, which are generally observed in random structures, appeared along the entire length of the peptides. In contrast, several NMR parameters indicate that peptides are better structured in dodecylphosphocholine (DPC) solution and that they share very similar conformations. In particular, H_α resonances (Tables S6-S9), and many NOE signals clearly point to a folded structure encompassing the N-terminal residues (1-5) and extended

Accepted Article

conformation of residues 6-8 (6-7 for **1** and **16**). Non-trivial medium range NOE interactions, among which $d_{\alpha N}(i, i+2)$ 1-3, 2-4, 3-5, $d_{NN}(i, i+2)$ 2-4, and $d_{\alpha N}(i, i+3)$ 1-4, are observed pointing to a turn-helical structure along residues 1-5. Low temperature coefficient of the backbone amide proton of residue 4 ($-\Delta\delta/\Delta T \sim 4$ ppb/K) confirms this hypothesis. C-terminal region is in extended conformation as indicated by the strong $d_{\alpha N}(i, i+1)$ NOEs and large $^3J_{HN\text{-}H\alpha}$ coupling constants. Finally, NOE contacts between Arg4 and His6 side chains indicate that these are spatially close.

NOE distance restraints obtained for peptide **17** in DPC micelles (Table S10) were used as the input data for a simulated annealing structure calculation using the program DYANA.[43] Superposition of the 10 lowest energy conformers of **17** is shown in Figure 2. The root mean square deviation (RMSD) to the average structure for backbone heavy atoms is 0.31 Å. Since a β-turn may be defined as four consecutive non-helical residues that have a Cα(i)-Cα(i+3) distance < 7 Å, two *β*-turns that involve Gly1 to Arg4 and Leu2 to *D*-Ala5, can be identified.

The first β-turn structure is stabilized by a hydrogen bond between the carbonyl oxygen of Gly1 and the amide hydrogen of Arg4. Residues 6 and 7 are in extended conformations, residue 8 is more flexible. The side chain are also well defined, the RMSD for all heavy atoms is 0.74 Å. The side chains of Arg4 and His6 are close and form a positively charged hydrophilic surface while Leu2 and Leu3 side chains establish a hydrophobic surface pointing in the opposite direction. By the way, to investigate the protonation state of the histidine side chain in DPC solution, proton spectra were recorded for peptide **17** at different pH values. In particular, we followed the chemical shift variation of Hδ and Hε of His^6. An upfield shift was observed for both proton signals upon variation of the pH from 2 to 8 (Figure S1). The observed chemical shift changes were the result of the dynamic equilibrium between a charged and noncharged His^6 imidazole group. Following this chemical shift variation, we could determine an apparent pK_a value for the imidazole group. This pK_a value is 6.65±0.04. Hence, the His^6 imidazole group is in equilibrium between the charged and uncharged states at physiological pH (7.4), with a prevalence (about 5-fold) of the uncharged state.

Accepted Article

Finally, the sequential $d_{\alpha N}$(i, i+1) NOEs between Leu2-Leu3, and Leu3-Arg4 indicative of extended/random conformations are consistently violated by the turn structures (violations of about 0.20 Å). It can be hypothesized the existence of a conformational equilibrium between the turns and less defined structures for these peptides.

DISCUSSION

In the present study, we performed a SAR study and a NMR conformational analysis of peptides **1** and **2** which are able to selectively inhibit GRK2.[35] Ala-scan results (Table 2) indicated that, while C-terminal residues are important for the activity of both peptides, N-terminal residues Leu2 and Leu3 are important only for the shorter peptide **1**. Since the conformational preferences in solution of the two peptides are very similar, a possible explanation of the different SAR observed is that hydrophobic interaction of residues Leu2 and Leu3 with the target are borrowed by Ile8 in peptide **2** (Ile8 is lacking in peptide **1**). Arg4 side chain is of little importance for the activity of both the peptides, in contrast, replacement of Arg5 with Ala completely abolishes the inhibitory activity. Since in the original sequence, the amino acid in position 5 is a *D*-enantiomer, *D*-Arg5 was substituted by *D*-Ala, in order to discern the real role of molecular orientation from the effects of the amino acid side chain on the inhibitory activity. We found that substitution with a neutral *D*-amino acid such as alanine does not change the inhibitory properties of peptides **1** and **2**, thus suggesting an important role for the chirality of amino acid 5 rather than for the side chain. Interestingly, both side chains of Arg4 and *D*-Arg5 can be replaced by a neutral amino acid when the chirality is retained. Indeed, peptide **17** (*D*-Ala derivative of peptide **2**) showed the highest GRK2 inhibition potency of the series. These peptides retain specificity for the GRK2 since they were equally effective on GRK2 using two different substrates. Also, they keep selectivity since they are ineffective in inhibition GRK5 activity on the same substrates.

Peptide **1**, **2**, **17** ability to increment basal and βAR stimulated cAMP production in HEK-293 cells is consistent with their effective inhibition of GRK2 (Figure 1). However, the low entity of those increments is likely due to the difficulty of the peptides to cross the cell membrane. The slight higher activity of peptide **2** compared to **1** roughly parallels its higher GRK2 inhibition potency. Differently, slight higher activity of peptide **2** compared to **17** would indicate that, even if *D*-Arg5 is dispensable for GRK2 interaction (Table 2), it can improve the permeating properties of the peptide. NMR analysis of peptides **1**, **2**, **16**, and **17** was performed in water and DPC micelle solutions. The last is a membrane mimetic medium and was chosen since GRK2 phosphorylation of GPCRs occurs close to the plasma membrane. Peptides conformational preferences are similar since they have similar diagnostic NMR parameters. Peptides structures in DPC micelles are characterized by two *β*-turns that involve Gly1 to Arg4 and Leu2 to *D*-Ala5 (or *D*-Arg5), followed by a short extended region encompassing residues 6 and 7 (Figure 2). The NMR structures of the peptides in DPC are very similar to the X-ray structure of the fragment encompassing the HJ loop of the GRK2 (pdb entry 3CIK)[44] which, indeed, was the starting point for the design of the peptides **1** and **2**.[35] Figure 3 shows the superposition of the NMR structure of **17** with that of the fragment 383-390 of the GRK2. Equivalent backbone atoms of **17** and GRK2 superimpose to an RMSD of 1.00 Å. It can be also observed the good overlapping of the unchanged side chains which occupies similar space regions. Therefore, the isolated peptide keeps the 3D structure of the protein segment and likely competes with the activation functions of this loop.[33,34] This result could explain the selectivity observed for these peptides towards GRK2 compared to GRK5. In fact, GRK5 HJ loop corresponding sequence is MIEGQS (CLUSTAL Omega alignment; www.ebi.ac.uk/Tools/msa/clustalo) which compared to the GRK2 sequence LLRGHS has, *inter alia*, a very different charge content (-1 vs +1/+2).

CONCLUSION

Accepted Article

GRK2 is involved in the regulation of many pivotal cell functions, and is therefore a key player in human health and diseases, such as definite pathological cardiovascular processes. Hence, modulation of its activity could be exploited with therapeutic purposes. The present study describes the synthesis, SAR study and conformational analysis of two HJ-loop derived peptides which are able to selectively inhibit GRK2. Starting from peptides **1** and **2**, previously described, this study: i) found the (in)dispensable residues which can be replaced in an attempt to improve peptide properties (GRK2 interaction, membrane permeation); ii) determined their conformational preferences which can help the design of novel peptides and peptido-mimetics with enhanced conformational stability. These steps are currently in progress in our lab.

EXPERIMENTAL SECTION

Synthesis.

The synthesis of GRK2 analogues was performed according to the solid phase approach using standard Fmoc methodology in a manual reaction vessel.[37] N^{α}-Fmoc-protected amino acids, Rinkamide-resin, N-hydroxy-benzotriazole (HOBt), 2-(1H-benzotriazole-1-yl)-1,1,3,3-tetramethyluronium hexafluoro-phosphate (HBTU), N,N-diisopropylethyl-amine (DIPEA), Piperidine and Trifluoroacetic acid were purchased from Iris Biotech (Germany). Peptide synthesis solvents, reagents, as well as CH_3CN for high performance liquid chromatography (HPLC) were reagent grade and were acquired from commercial sources and used without further purification unless otherwise noted. The first amino acid, N^{α}Fmoc-Xaa-OH (Xaa = Ile, Ser(tBu), Ala), was linked on to the Rink resin (100–200 mesh, 1% DVB, 0.75 mmol/g) previously deprotected by a 25% piperidine solution in N,N-dimethylformamide (DMF) for 30 min.

The following protected amino acids were then added stepwise: N^{α}-Fmoc-Ala-OH, N^{α}-Fmoc-His($N_{(im)}$trityl(trityl(Trt))-OH, N^{α}-Fmoc-DArg(2,2,4,6,7–pentamethyldihydro benzofuran-5-sulfonyl (Pbf))-OH (or N^{α}-Fmoc-DAla-OH) N^{α}-Fmoc-Arg(Pbf)-OH, N^{α}-Fmoc-Leu-OH, N^{α}-Fmoc-Gly-OH. Each coupling reaction was accomplished using a 3-fold excess of amino acid with HBTU and

Accepted Article

HOBt in the presence of DIPEA (6 eq.). The N^{α}-Fmoc protecting groups was removed by treating the protected peptide resin with a 25% solution of piperidine in DMF (1x 5 min and 1x 25 min). The peptide resin was washed three times with DMF, and the next coupling step was initiated in a stepwise manner. The peptide resin was washed with dichloromethane (DCM)(3×), DMF (3×), and DCM (3×), and the deprotection protocol was repeated after each coupling step.

In addition, after each step of deprotection and after each coupling step, Kaiser test was performed to confirm the complete removal of the Fmoc protecting group, respectively, and to verify that complete coupling has occurred on all the free amines on the resin.

The N-terminal Fmoc group was removed as described above, and the peptide was released from the resin with trifluoroacetic acid (TFA) / triisopropylsilane(iPr_3SiH) /H_2O (90:5:5) for 3 h. The resin was removed by filtration, and the crude peptide was recovered by precipitation with cold anhydrous ethyl ether to give a white powder and then lyophilized.

Purification and characterization. All crude peptides were purified by reversed-phase high performance liquid chromatography (RP-HPLC) on a semipreparative C18-bonded silica column (Phenomenex, Jupiter, 250×10mm) using a Shimadzu SPD 10A UV/VIS detector, with detection at 210 and 254 nm.

The column was perfused at a flow rate of 3 ml/min over 40 min with solvent A (10%, v/ v, water in 0.1% aqueous TFA), and a linear gradient from 10 to 90% of solvent B (80%, v/v, acetonitrile in 0.1% aqueous TFA). Analytical purity and retention time (t_R) of each peptide were determined using HPLC conditions in the above solvent system (solvents A and B) programmed at a flow rate of 1 mL/min using a linear gradient from 10 to 90% B over 25 min, fitted with C-18 column Phenomenex, Juppiter C-18 column (250× 4,60mm; 5µ).

All analogues showed >97% purity when monitored at 215 nm. Homogeneous fractions, as established using analytical HPLC, were pooled and lyophilized.

Peptides molecular weights were determined by electrospray ionization mass spectrometry. ESI-MS analysis in positive ion mode, were made using a Finnigan liquid chromatography quadrupole

Accepted Article

mass spectrometry (LCQ) ion trap instrument, manufactured by Thermo Finnigan (San Jose, CA, USA), equipped with the Excalibur software for processing the data acquired. The sample was dissolved in a mixture of water and methanol (50/50) and injected directly into the electrospray source, using a syringe pump, which maintains constant flow at 5 µl /min. The temperature of the capillary was set at 220 °C

NMR Spectroscopy.

The samples for NMR spectroscopy were prepared by dissolving the appropriate amount of peptide to obtain a concentration 1-2 mM in 0.55 ml of $^{1}H_2O$ (pH 5.5), 0.05 ml of $^{2}H_2O$ for water samples, 200 mM DPC-d_{38} for micelle samples. NMR spectra were recorded on a Varian INOVA 700 MHz spectrometer equipped with a z-gradient 5 mm triple-resonance probe head. All the spectra were recorded at a temperature of 25 °C. The spectra were calibrated relative to 3-(trimethylsilanyl)propionic acid (TSP, 0.00 ppm) as internal standard. One-dimensional (1D) NMR spectra were recorded in the Fourier mode with quadrature detection. Water suppression was achieved by using the double-pulsed field gradient spin-echo (DPFGSE) scheme.[45] 2D double quantum filtered correlated spectroscopy (DQF-COSY),[46] TOCSY,[47] and NOESY[48] spectra were recorded in the phase-sensitive mode using the method of States.[49] Data block sizes were 2048 addresses in t_2 and 512 equidistant t_1 values. Before Fourier transformation, the time domain data matrices were multiplied by shifted $\sin^2$ functions in both dimensions. A mixing time of 70 ms was used for the TOCSY experiments. NOESY experiments were run with mixing times in the range of 100-200 ms. The qualitative and quantitative analyses of DQF-COSY, TOCSY, and NOESY spectra, were obtained using the interactive program package XEASY.[50] $^{3}J_{\mathrm{HN\text{-}H\alpha}}$ coupling constants were obtained from 1D ^{1}H NMR and 2D DQF-COSY spectra. Many $^{3}J_{\mathrm{HN\text{-}H\alpha}}$ coupling constants were difficult to measure in DPC solution probably because of a combination of small coupling constants and broad lines. The temperature coefficients of the amide proton chemical shifts were

Accepted Article

calculated from 1D ^{1}H NMR and 2D TOCSY experiments performed at different temperatures by means of linear regression.

Structural Determinations.

The NOE-based distance restraints were obtained from NOESY spectra collected with a mixing time of 200 ms. The NOE cross peaks were integrated with the XEASY program and were converted into upper distance bounds using the CALIBA program incorporated into the program package DYANA.[43] Cross peaks which overlapped more than 50% were treated as weak restraints in the DYANA calculation. For each examined peptide, an ensemble of 100 structures was generated with the simulated annealing of the program DYANA. An error-tolerant target function (tf-type=3) was used to account for the peptide intrinsic flexibility of the peptide. The annealing procedure produced 100 conformations from which 20 structures were chosen, whose interprotonic distances best fitted NOE derived distances, and then refined through successive steps of restrained and unrestrained EM calculations using the Discover algorithm (Accelrys, San Diego, CA) and the consistent valence force field (CVFF)[51] as previously described. Graphical representation were carried out with the the UCSF Chimera package.[52] RMS deviation analysis between energy minimized structures were carried out with the program MOLMOL.[53]

***In Vitro* Methods**

GRK Activity in Rhodopsin Phosphorylation Assays. To evaluate the effect of all synthesized peptides on GRK2 activity we assessed GRK2 or GRK5 purified proteins by light-dependent phosphorylation of rhodopsin-enriched rod outer segment membranes (ROS) using [γ-^{32}P]-ATP as previously described.[22,54] Briefly, 50 ng of active GRK2 or GRK5 were incubated with ROS membranes in presence or absence of inhibitor peptides in reaction buffer (25 µl) containing 10 mM $MgCl_2$, 20 mM Tris-Cl, 2 mM ethylenediaminetetraacetic acid (EDTA), 5 mM ethylene glycol tetraacetic acid (EGTA), and 0.1 mM ATP and 10 Ci of [γ-^{32}P]-ATP. After incubation with white

Accepted Article

light for 15 minutes at room temperature, the reaction was quenched with ice-cold lysis buffer and centrifuged for 15 minutes at 13000*g*. The pelleted material was resuspended in 35 μL protein gel loading dye, electrophorosed and resolved on SDSPAGE 4-12% gradient (Invitrogen), stained with Coomassie blue, destained, vacuum dried, and exposed for autoradiography. Phosphorylated rhodopsin was visualized by autoradiography of dried gels and quantified using a PhosphorImager (Molecular Dynamics). Alternatively, the pellet was resuspended in 100 μL of ice-cold lysis buffer and the level of [γ-^{32}P]-ATP incorporation into ROS was determined by liquid scintillation counter.

MBP Kinase assay. 50 ng of active GRK2 or GRK5were assayed on 100 ng of purified MBP in presence or absence of peptides **1-17**. Phosphorylation reactions were initiated by adding 20 mM ATP, 1 mM $CaCl_2$, 20 mM $MgCl_2$, 4 mM Tris, pH 7.5, and 10 Ci of [γ-^{32}P]-ATP (specific activity 3000 Ci/mmol) and prolonged for 30 min at 37°C. Laemmli buffer was added to stop the reaction. Sample were processed as above described.[12]

cAMP synthesis. HEK 293 overexpressing β_2AR were plated in 96-well plates (10,000 cells/well) and serum starved overnight. Cells were incubated in a fresh medium in the presence **2** and **22** peptides 1 μM for one hour and then stimulated with non selective β adrenergic receptor agonist Isoproterenol 10 μM for 15 min. The cAMP quantification was evaluated by enzyme immunoassay, using an EIA commercial kit (RPN 2255 GE Healthcare Bio-Sciences AB, Uppsala, Sweden). The cAMP content present in HEK- 293 cell was expressed in fmoles per well. All values are presented as mean ± SEM of three independent experiments. One-way ANOVA was performed to compare the different groups. A significance level of $P<0.05$ was assumed for all statistical evaluations. Statistics were computed with GraphPad Prism Software (GraphPad Software Inc., version 4, San Diego, CA, USA).

Supporting Information. NMR data of the analyzed peptides.

Accepted Article

Accepted Article

ACKNOWLEDGMENT. The LC-MS and NMR spectral data were provided by Centro di Servizio Interdipartimentale di Analisi Strumentale (CSIAS), Università degli Studi di Napoli "Federico II". The assistance of the staff is gratefully appreciated. We thank Dr Linda Piras for many helpful discussions.

REFERENCES

1. Pitcher, J. A.; Freedman, N. J.; Lefkowitz, R. J Annu Rev Biochem 1998, 67, 653–692.
2. Ferguson, S. S. Pharmacol Rev 2001, 53, 1–24.
3. Reiter, E.; Lefkowitz, R. J. Trends Endocrinol Metab 2006, 17, 159–165.
4. (a) Moore, C. A.; Milano, S. K.; Benovic, J. L. Annu Rev Physiol 2007, 69, 451–482. (b) Hupfeld, C. J.; Olefsky, J. M. Annu Rev Physiol 2007, 69, 561–577
5. Ribas, C.; Penela, P.; Murga, C.; Salcedo, A.; Garcia-Hoz, C.; Juradopueyo, M.; Aymerich, I. And Mayor, F. Jr. Biochim Biophys Acta 2007, 1768, 913-922.
6. Oppermann, M.; Diverse-Pierluissi, M.; Drazner, M.H.; Dyer, S.L.; Freedman, N.J.; Peppel, K.C.; Lefkowitz, R. J. Proc Natl Acad Sci U.S.A. 1996, 93, 7649–7654.
7. Willets, J. M.; Challiss, R. A. J.; Nahorski, S. R. Trends Pharmacol Sci 2003, 24, 626-633.
8. Inglesef, J.; Freedman, N. J.; Koch, W. J.; Lefkowit, R. J. J Biol Chem 1993, 268, 23735-23738
9. Penela, P.; Murga, C.; Ribas,C.; Lafarga, V Mayor, F. Jr. Br J Pharmacol 2010, 160, 821–832.
10. Jurado-Pueyo, M.; Campos, P. M., Mayor F., Murga C. GRK2-dependent desensitization downstream of G proteins. J. Recept. Signal Transduct. Res. 2008, 28, 59–70.
11. Evron, T.; Daigle, T. L.; Caron. M. G. Trends Pharmacol Sci 2012, 33, 154-164.
12. Cipolletta, E.; Campanile, A.; Santulli, G.; Sanzari, E.; Leosco, D.; Campiglia, P.; Trimarco, B.; Iaccarino, G. Cardiovasc Res 2009, 84, 407–415
13. Matkovich SJ, Diwan A, Klanke JL, Hammer DJ, Marreez Y, Odley AM, Brunskill EW, Koch WJ, Schwartz RJ, Dorn GW. Circ Res 2006, 99: 996–1003.
14. Penela P, Rivas V, Salcedo A, Mayor F Jr. Proc Natl Acad Sci USA 2010, 107: 1118–1123
15. Vroon A, Heijnen CJ, Kavelaars A. J Leukoc Biol 2006, 80, 1214–1221.
16. Penela, P.; Ribas, C.; Aymerich, I.; Mayor, Jr, F. Cell Adh Migr.2009, 3: 19–23.

17. Ferguson, S. S. Trends Pharmacol Sci 2007, 28, 173–179.
18. Metaye, T., Gibelin, H.; Perdrisot, R.; Kraimps, J.L. Cell Signal 2005, 17, 917–928.
19. Ungerer, M.; Kessebohm, K.; Kronsbein, K.; Lohse, M. J.; Richardt, G. Circ Res 1996, 79, 455-460.
20. Choi, D. J.; Koch, W. J.; Hunter, J. J.; Rockman, H. A. J Biol Chem. 1997, 272, 17223-17229.
21. Gros, R.; Benovic, J. L.; Tan, C. M.; Feldman, R. D. J Clin Invest 1997, 99, 2087-2093.
22. Iaccarino, G.; Barbato, E.; Cipolletta, E.; De Amicis, V.; Margulies, K. B.; Leosco, D.; Trimarco, B.; Koch, W. J. Eur Heart J 2005, 26, 1752-1758
23. Harris, C. A.; Chuang, T. T.; Scorer, C. A. Basic Res Cardiol 2001, 96, 364-368.
24. Yi, X. P.; Gerdes, A. M.; Li, F. Hypertension 2002, 39, 1058-1063.
25. Vroon, A.; Kavelaars, A.; Limmroth, V.; Lombardi, M. S.; Goebel, M. U.; Van Dam, A. M.; Caron, M. G.; Schedlowski, M.; Heijnen, C. J. J Immunol 2005, 174: 4400-4406.
26. Dorsam, R. T.; Gutkind, J. S. Nat Rev Cancer. 2007;7:79–94
27. Lefkowitz, R. J. Nat. Biotechnol. 1996, 14, 283–286.
28. Iaccarino, G.; Koch, W.J. Expert Opin Investig Drugs 1999, 8, 545–554. b) Rengo, G.; Lymperopoulos, A.; Leosco, D.; Koch W. J. J Mol Cell Cardiol. 2011, 50, 785–792.
29. Setyawan, J.; Koide, K.; Diller, T. C.; Bunnage, M. E.; Taylor, S.; Nicolai, K. C.; Brunton, L. L. Mol Pharmacol 1999, 56, 370-376.
30. Iino, M.; Furugori, T.; Mori, T.; Moriyama, S.; Fukuzawa, A., Shibano, T. J Med Chem 2002, 45, 2150-2159.
31. Benovic, J. L.; Stone, W. C.; Caron, M. G.; Lefkowitz, R. J. J Biol Chem 1989, 264, 6707-6710.
32. Takeda Pharmaceuticals Company Limited, Ikeda, S., kaneko, M., Fujiwara, S. World patent WO2007034846.
33. Winstel, R.; Ihlenfeldt, H. G.; Jung, G.; Krasel, C.; Lohse, M. J. Biochem Pharmacol 2005, 70, 1001–1008.
34. Niv, M. Y.; Rubin, H.; Cohen, J.; Tsirulnikov, L.; Licht, T.; Peretzman-Shemer, A.; Cna'an, E.; Tartakovsky, A.; Stein, I.; Albeck, S.; Weinstein, I.; Goldenberg-Furmanov, M.; Tobi, D.; Cohen, E.; Laster, M.; Ben-Sasson, S. A.; Reuveni, H. J Biol Chem 2004, 279, 1242–1255.
35. Anis, Y.; Leshem, O.; Reuveni, H.; Wexler, I.; Ben Sasson, R.; Yahalom, B.; Laster, M.; Raz I., Ben Sasson, S., Shafrir, E.; Ziv, E. Diabetologia, 2004, 47, 1232–1244.
36. Mayer, G.; Wulffen, B.; Huber, C.; Brockmann, J.; Flicke, B.; Neumann, L.; Hafenbradl, D.; Kleb, B. M.; Lohse, M. J.; Krasel, C.; Blind, M. RNA 2008, 14, 524–534.

Accepted Article

Accepted Article

37. Atherton, E.; Sheppard, R. C. Solid-Phase Peptide Synthesis: A Practical Approach; IRL Press: Oxford, U.K., 1989.
38. Palczewski, K.; Buczylko, J.; Kaplan, M. W.; Polans, A. S.; Crabb, J. W. J Biol Chem 1991, 266, 12949-12955.
39. Ohguro, H.; Palczewski, K.; Ericsson, L.H.; Walsh, K.A.; Johnson, R.S. Biochemistry 1993, 32, 5718-5724.
40. Kishimoto, A.; Nishiyama, K.; Nakanishi, H.; Uratsujig, Y.; Nomura, H.; Takeyama, Y.; Nishizuka, Y. J Biol Chem Vol. 1985, 260, 12492-12499.
41. Wüthrich, K. NMR of Proteins and nucleic acids; Wiley-Interscience: New York, 1986.
42. Wishart, D.S.; Sykes, B.D.; Richards, F.M. Biochemistry 1992, 31, 1647-1651. b) Andersen, N.H.; Liu, Z.; Prickett, K.S. FEBS Lett 1996, 399, 47-52.
43. Güntert, P.; Mumenthaler, C.; Wüthrich, K. J Mol Biol1997, 273, 283-298.
44. Tesmer, J. J .G.; Tesmer, V. M.; David T.; Lodowski, D.T.; Steinhagen, H.; Huber, J. J Med Chem 2010, 53, 1867–1870.
45. Hwang, T.L.; Shaka, A. J Magn Reson 1995, 112, 275-279.
46. Piantini, U.; Sorensen, O.; W.; Ernst R.R. J Am Chem Soc 1982, 104, 6800-6801.
47. Braunschweiler, L.; Ernst, R. R. J Magn Reson 1983, 53, 521-528.
48. Jeener, J.; Meier, B.H.; Bachman, P.; Ernst R.R. J Chem Phys 1979, 71, 4546-4553.
49. States, D.J.; Haberkorn, R.A.; Ruben D.J. J Magn Reson 1982, 48, 286-292.
50. Bartels, C.; Xia, T.; Billeter, M.; Güntert, P.; Wüthrich, K. J Biomol NMR 1995, 6, 1-10.
51. Maple, J. R.; Dinur, U.; Hagler, A. T. Proc Natl Acad Sci USA. 1988, 85, 5350-5354.
52. Pettersen, E.F.; Goddard, T.D.; Huang, C.C.; Couch, G.S.; Greenblatt, D.M.; Meng, E.C.; Ferrin, T.E. J Comput Chem 2004, 25, 1605-1612.
53. Koradi, R., Billeter, M., Wüthrich, K. MOLMOL: J Mol Graph 1996, 14, 51-55.
54. Cho, M-C.; Rao, M.; Koch, W. J.; Thomas, S. A.; Palmiter, R, D.; Rockman, H. A. Circulation 1999, 99, 2702-2707.

Figure Captions

Figure 1. cAMP production in HEK-293 cells treated with **1**, **2** and **17** as determines by enzyme immunoassay. ISO: Isoproterenol. Each data point represents the mean±SEM of 3 independent experiments; * = $p<0.0001$ *vs* Ctr; # = $p<0.01$ *vs* Iso.

Figure 2. Stereoview of the 10 lowest energy conformers of **17**. Structures were superimposed using the backbone heavy atoms. Heavy atoms are shown with different colours (carbon, green; nitrogen, blue; oxygen, red). Hydrogen atoms are not shown for clarity.

Figure 3. Stereoview of **17** lowest energy conformer (green) and fragment 383-390 of GRK2 (yellow, pdb entry 3CIK). The structures are superimposed using the backbone heavy atoms. Structure orientation is the same as in Figure 2.

Accepted Article

Accepted Article

Table 1. Different peptide fragments considered in this study.

Peptide		Sequences							
$^{383\text{-}390}$HJ loop GRK2		K	L	L	R	G	H	S	P
KRX-683$_{107}$	Myristyl	G	L	L	R	r	H	S	
KRX-683$_{124}$	Lauryl	G	L	L	R	r	H	S	I
1		G	L	L	R	r	H	S	
2		G	L	L	R	r	H	S	I

Accepted Article

Table 2. Structure and inhibition activities of linear peptides **1-17**

Peptide	Sequence	GRK2 Inhib. (%±SD)[a]		GRK5 Inhib. (%±SD)[a]	
		ROS[b]	MBP[c]	ROS	MBP
1	GLLRrHS	47.6±5.5	54.2±6.1	<5	<5
3	G**A**LRrHS	<5	<5	<5	<5
4	GL**A**RrHS	<5	<5	<5	<5
5	GLL**A**rHS	42.2±9.7	38.2±4.5	<5	<5
6	GLLR**A**HS	<5	<5	<5	<5
7	GLLRr**A**S	13.5±6.4	25.6±5.7	<5	<5
8	GLLRrH**A**	22.3±5.4	28.8±9.2	<5	<5
2	GLLRrHSI	49.6±6.3	60.2±5.0	<5	<5
9	G**A**LRrHSI	45.7±12.3	54.5±9.1	<5	<5
10	GL**A**RrHSI	46.6±12.3	47.7±7.2	<5	<5
11	GLL**A**rHSI	45.7±6.2	42.1±7.8	<5	<5
12	GLLR**A**HSI	<5	<5	<5	<5
13	GLLRr**A**SI	<5	<5	<5	<5
14	GLLRrH**A**I	<5	<5	<5	<5
15	GLLRrHS**A**	<5	<5	<5	<5
16	GLLR**a**HS	55.5±4.7	54.2±3.2	<5	<5
17	GLLR**a**HSI	63.2±9.7	55.5±6.0	<5	<5

[a]Data represent mean values (±SD) of three independent determinations. [b]GRK2 and GRK5 purified protein activities (50 ng) were tested on rod outer segments (ROS) in presence or absence of 1 μM inhibitors. [c] GRK2 and GRK5 purified protein activities (50 ng) were tested on Myelin Basic Protein (MBP) in presence or absence of 1 μM inhibitors.

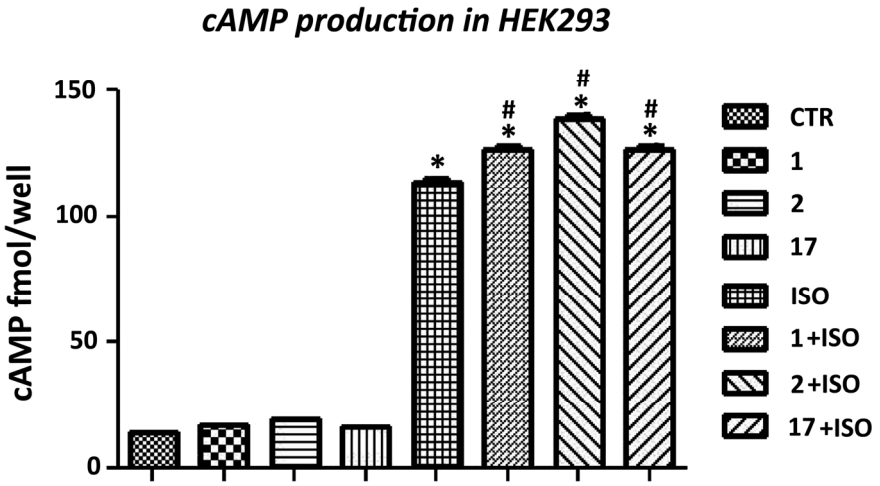

cAMP production in HEK-293 cells treated with 1, 2 and 17 as determines by enzyme immunoassay. ISO: Isoproterenol. Each data point represents the mean±SEM of 3 independent experiments; * = p<0.0001 vs Ctr; # = p<0.01 vs Iso.
89x57mm (600 x 600 DPI)

Accepted

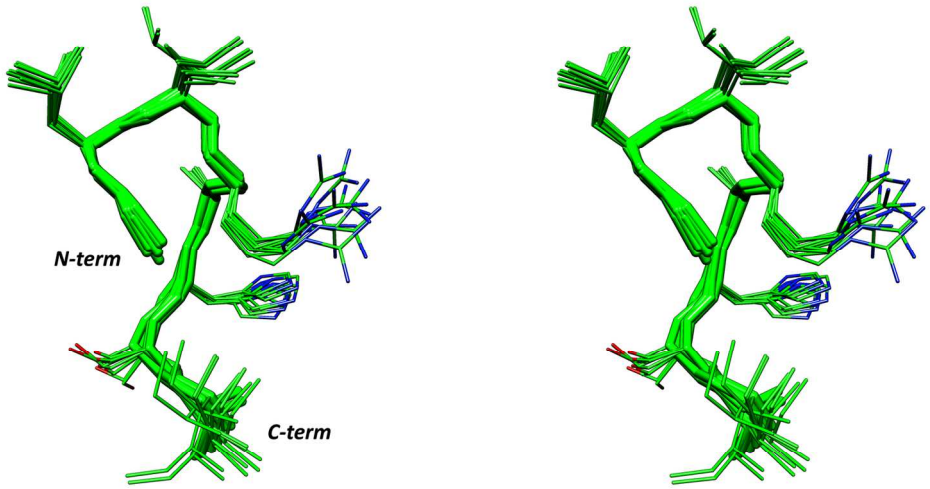

Stereoview of the 10 lowest energy conformers of 17. Structures were superimposed using the backbone heavy atoms. Heavy atoms are shown with different colours (carbon, green; nitrogen, blue; oxygen, red). Hydrogen atoms are not shown for clarity.
150x91mm (300 x 300 DPI)

Accepted

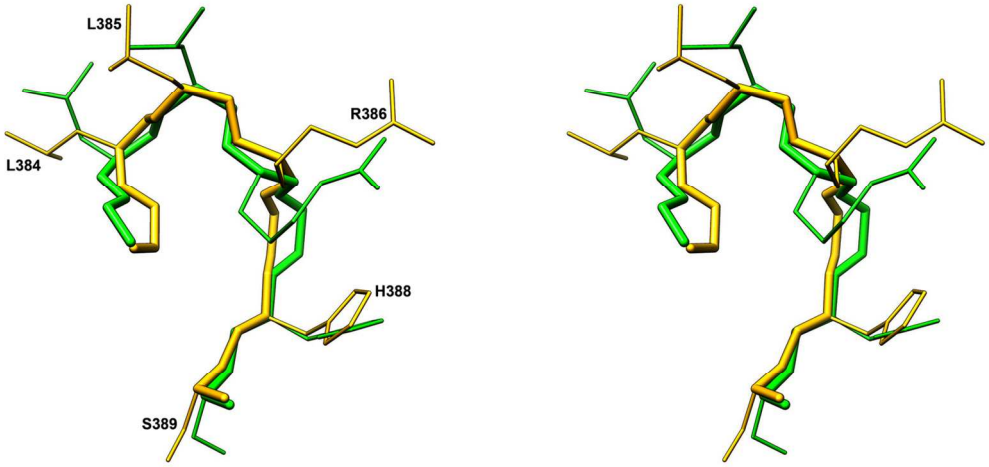

Stereoview of 17 lowest energy conformer (green) and fragment 383-390 of GRK2 (yellow, pdb entry 3CIK). The structures are superimposed using the backbone heavy atoms. Structure orientation is the same as in Figure 2.
129x60mm (300 x 300 DPI)

Accepted